ACS APPLIED MATERIALS & INTERFACES

Research Article

www.acsami.org

New Star-Shaped Carriers Composed of β-Cyclodextrin Cores and Disulfide-Linked Poly(glycidyl methacrylate) Derivative Arms with Plentiful Flanking Secondary Amine and Hydroxyl Groups for Highly Efficient Gene Delivery

Y. Hu, Y. Zhu, W.T. Yang, and F. J. Xu*

State Key Laboratory of Chemical Resource Engineering, Key Laboratory of Carbon Fiber and Functional Polymers, Ministry of Education, College of Materials Science & Engineering, Beijing University of Chemical Technology, Beijing 100029 China

ABSTRACT: The biocleavable star-shaped vectors (CD-SS-PGEAs) consisting of nonionic β-cyclodextrin (β-CD) cores and disulfide-linked low-molecular-weight poly(glycidyl methacrylate) (PGMA) derivative arms with plentiful flanking secondary amine and hydroxyl groups were successfully proposed for highly efficient gene delivery. A simple two-step method was first adopted to introduce reduction-sensitive disulfide-linked initiation sites of atom transfer radical polymerization (ATRP) onto β-CD cores. The disulfide-linked PGMA arms prepared subsequently via ATRP were functionalized via the ring-opening reaction with ethanolamine (EA) to produce the cationic EA-functionalized PGMA (PGEA) arms with plentiful secondary amine and nonionic hydroxyl units. The cationic PGEA arms can be readily cleavable from the β-CD cores under reducible conditions. Such biocleavable star-shaped CD-SS-PGEA vectors possessed the good pDNA condensation ability, low cytotoxicity, and efficient gene delivery ability.

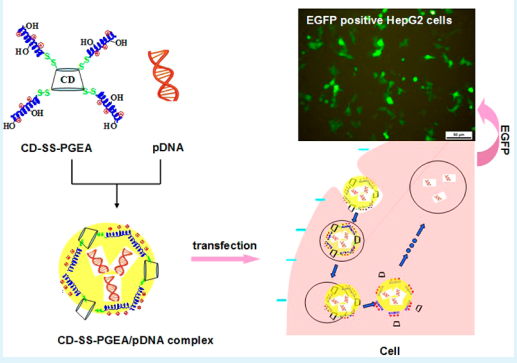

KEYWORDS: *gene delivery, bioreducible vector, PGEA, β-cyclodextrin, ATRP*

INTRODUCTION

It is of crucial importance to design gene delivery vectors with low cytotoxicity and high transfection efficiency.[1,2] In comparison with viral vectors and cationic lipids, cationic polymers as the major type of nonviral gene delivery vectors show low host immunogenicity and can be produced on a large scale. A large number of polycations, including polyethylenimine (PEI),[3] polyamidoamine,[4,5] chitosan,[6] and cyclodextrin (CD)-based cationic carriers,[7−10] have been reported to deliver nucleic acids. CDs are a series of cyclic oligosaccharides composed of 6, 7, or 8 D(+)-glucose units linked by α-1,4-linkages and named α-, β-, or γ-CD, respectively. The use of CD derivates as gene vector is particularly appealing because of their excellent biocompatibility, nonimmunogenicity, and low toxicity in animal and human bodies.[11] A class of CD-based cationic polymers has been introduced for the efficient delivery of nucleic acids.[7,9,10,12−14]

Star-shaped cationic polymers have recently attracted considerable attention as non-viral gene carriers because of their dense molecular architecture with moderate flexibility.[15,16] Novel star-shaped gene carriers using CDs as cores could be developed when the hydroxyl groups on the outside surfaces of CDs are derivatized to serve as initiation sites for growing cationic branches.[15,17,18] Atom transfer radical polymerization (ATRP) is a recently developed "controlled" radical polymerization method, which has been used to prepare graft copolymers from some polysaccharides.[19−21] In particular, the successful ATRP syntheses of star-shaped copolymers composed of β-CD cores and cationic poly((2-dimethyl amino)ethyl methacrylate) (or PDMAEMA) arms provide a versatile means for designing well-controlled star carriers.[15] However, the high cytotoxicity of PDMAEMA-based vectors limits their effective applications.

We found that ethanolamine (EA)-functionalized poly(glycidyl methacrylate) (PGMA), or PGEA with plentiful flanking secondary amine and hydroxyl groups, can produce good transfection efficiency in some cell lines, while exhibiting low toxicity.[22] It was noted that the linear PGEA vector was non-degradable and its good transfection efficiency was dependent on the high molecular weights. More recently, the high-molecular-weight comb-shaped PGEA (c-PGEA) vectors composed of the low-molecular-weight PGEA backbone and side chains were proposed by a combination of ATRP and ring-opening reactions.[23] The PGEA side chains were linked with the PGEA backbones via hydrolyzable ester bonds. Such comb-shaped c-PGEA vectors possessed the partial degradability, which would benefit the final removal of PGEA from the body.

Reduction-sensitive polymers could be elegantly applied for intracellular triggered gene delivery.[24−26] The design rationale of bioreducible polymers usually involves incorporation of easy

Received: October 8, 2012
Accepted: December 27, 2012
Published: December 27, 2012

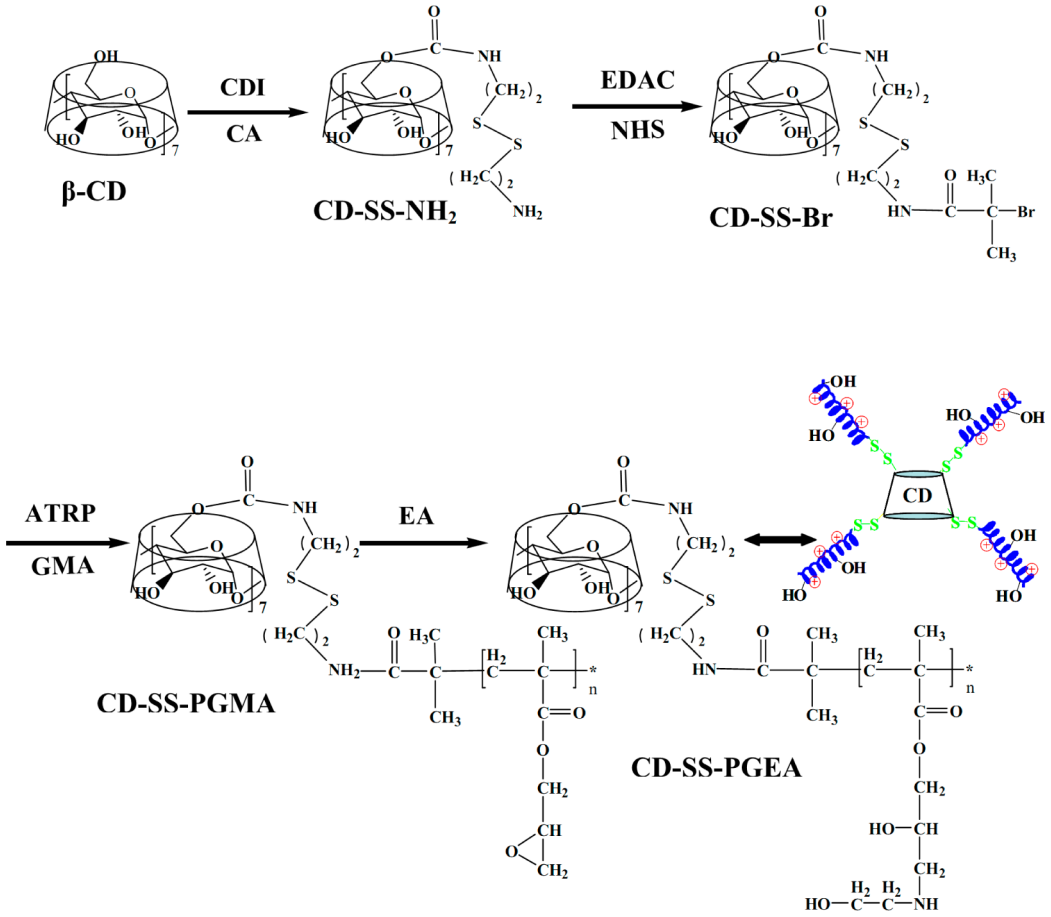

Figure 1. Schematic diagram illustrating the preparation processes of biocleavable CD-SS-PGEA vectors via ATRP. Functionalization of the primary hydroxyl group at carbon 6 is illustrated, but functionalization can also occur at any of the secondary hydroxyl groups.

intracellular reversible disulfide linkage(s). The intracellular reductive degradation arising from the disulfide linkages in the polycation vectors could induce lower molecular weight species and remove the lateral stabilizing effect of the polycation coating, enabling efficient transcription of the plasmid DNA (pDNA).[25,26] In this work, the biocleavable star-shaped vectors (CD-SS-PGEAs) consisting of nonionic β-CD cores and disulfide-linked low-molecular-weight PGEA arms with plentiful secondary amine and hydroxyl groups were successfully proposed via ATRP to synergistically combine favorable properties of flexible CD-based star polymers, low toxic PGEA, and reduction-sensitive polymers. The good gene transfer abilities of such biocleavable CD-SS-PGEA vectors were characterized in detail through a series of experiments.

EXPERIMENTAL SECTION

Materials. β-Cyclodextrin (β-CD, 99%), branched polyethylenimine (PEI, M_w ~25KDa), 1,1′-carbonyldiimidazole (CDI, 97%), cystamine dihydrochloride (CA, >98%), ethanolamine (EA, >98%), 1-ethyl-3-(3-dimethylaminopropyl) carbodiimide hydrochloride (EDAC, 98%), *N*-hydroxysuccinimide (NHS, 98%), α-bromoisobutyric acid (BIBA, 98%), glycidyl methacrylate (GMA >98%), *N*,*N*,*N*′,*N*″,*N*‴-pentamethyl diethylenetriamine (PMDETA, 99%), and copper(I) bromide (CuBr, 99%) were obtained from Sigma-Aldrich Chemical Co., St. Louis, MO. GMA was used after removal of the inhibitors in a ready-to-use disposable inhibitor-removal column (Sigma-Aldrich). 3-(4,5-Dimethylthiazol-2yl)-2,5-diphenyl tetrazolium bromide (MTT), penicillin, and streptomycin were purchased from Sigma Chemical Co., St. Louis, MO. Hela and HepG2 cell lines were purchased from the American Type Culture Collection (ATCC, Rockville, MD).

Introduction of Biocleavable ATRP Initiation Sites. As shown in Figure 1, the introduction of the biocleavable ATRP initiation sites onto β-CD was carried out in two steps: (1) activation of hydroxyl groups of CD in the presence of CDI catalyst to react with cystamine and produce the disulfide bonds-contained CD (CD-SS-NH_2), and (2) reaction of amine groups of CD-SS-NH_2 with BIBA in the presence of EDAC and NHS to produce the bromoisobutylryl-terminated CD (CD-SS-Br). For the activation of hydroxyl groups of CD, 1.2 g of CDI and 1.0 g of β-CD were dissolved in 3 and 4 mL of anhydrous DMSO, respectively. The CDI solution was added dropwise at room temperature into the β-CD solution. The reaction was allowed to proceed at room temperature for 24 h. Then, 12 mL of DMSO solution containing cystamine dihydrochloride (3.30 g) and triethyleneamine (TEA, 2.5 mL) was added dropwise into the above CDI-activated β-CD solution. The reaction mixture was stirred at room temperature under a nitrogen atmosphere for 24 h to produce CD-SS-NH_2. The final reaction mixture was precipitated and washed with excess diethyl ether, prior to being redissolved in 20 mL of deionized water and dialyzed against deionized water (4 × 5 L) with dialysis membrane (MWCO, 1000 Da) at room temperature for 24 h. The final products were freeze-dried to produce about 1.0 g of CD-SS-NH_2.

The resultant CD-SS-Br was synthesized via the reaction of primary amine groups of CD-SS-NH_2 with BIBA in the presence of EDAC and NHS. BIBA (0.57 g, 3.41 mmol), EDAC (0.52 g, 2.73 mmol) and NHS (0.28 g, 2.73 mmol) were dissolved in 10 mL of DMF, and then 0.5 mL of TEA was added. The mixture was stirred at 37 °C for 4 h, and mixed with 1.0 g of CD-SS-NH_2 dissolved in 8 mL of DMF; 1.5 mL of TEA was then added and the reaction mixture was stirred for 48

dx.doi.org/10.1021/am302249x | ACS Appl. Mater. Interfaces 2013, 5, 703−712

h at 37°C. At the end of the reaction, the reaction mixture was precipitated with excess diethyl ether, prior to being redispersed in 20 mL of deionized water and dialyzed against deionized water (4 × 5 L) with dialysis membrane (MWCO, 1000 Da) at room temperature for 24 h. The final products were freeze-dried to produce about 0.75 g of CD-SS-Br.

Synthesis of Biocleavable Star-Shaped CD-SS-PGEA via ATRP. For the preparation of CD-SS-PGMA starlike polymers via ATRP, the molar feed ratio [GMA (4 mL)]:[CuBr]:[PMDETA] of 100:1:1.5 was used at room temperature in 6 ml of anhydrous DMSO containing 0.2 g of CD-SS-Br. The reaction was conducted in a 25 mL flask equipped with a magnetic stirrer and under the typical conditions for ATRP.[19,20] GMA, CD-SS-Br and PMDETA were introduced into the flask containing 6 mL of anhydrous DMSO, and the reaction mixture was degassed by bubbling nitrogen for 10 min. Then, CuBr was added into the mixture under a nitrogen atmosphere. The flask was then sealed with a rubber stopper under a nitrogen atmosphere. The polymerization was allowed to proceed under continuous stirring at room temperature from 5 to 30 min. The final reaction mixture was precipitated with excess methanol and washed with deionized water, prior to lyophilization. The CD-SS-PGMA yields from ATRP time of 5, 10, and 30 min are 0.56, 0.80, and 1.37 g, respectively.

For the preparation of CD-SS-PGEA, 0.2 g of CD-SS-PGMA was dissolved in 8 mL of DMF. 5 mL of ethanolamine (EA) and 1 mL of triethyleneamine were then added. The reaction mixture was stirred at 37°C for 5 days to produce CD-SS-PGEA (Figure 1). The final reaction mixture was precipitated with excess diethyl ether. The crude product was re-dissolved in 10 mL of deionized water and dialyzed against deionized water (4 × 5 L) with dialysis membrane (MWCO, 1000 Da) at room temperature for 24 h. The final products were freeze-dried to produce about 0.15 g of CD-SS-PGEA.

Polymer Characterization. The molecular weights of polymers were determined by gel permeation chromatography (GPC), chemical composition by X-ray photoelectron spectroscopy (XPS), and chemical structure by nuclear magnetic resonance (NMR) and Fourier transform infrared (FTIR) spectroscopy. GPC measurements of CD-SS-PGMA were performed on a Waters GPC system equipped with Waters Styragel columns, a Waters-2487 dual wavelength (λ) UV detector, and a Waters-2414 refractive index detector. THF was used as the eluent at a low flow rate of 0.5 mL/min at 25°C. Monodispersed poly(methyl methacrylate) standards were used to obtain a calibration curve. GPC measurements of CD-SS-PGEA were performed on a YL9100 GPC system equipped with a UV/Vis detector and Waters Ultrahydrogel 250 and Ultrahydrogel Linear columns. A pH 3.5 acetic buffer solution was used as the eluent at a low flow rate of 0.5 mL/min at 25 °C. Monodispersed poly(ethylene glycol) standards were used to obtain a calibration curve. The XPS measurements were performed on a Kratos AXIS HSi spectrometer equipped with a monochromatized AlK_α X-ray source (1486.6 eV photons), using the same procedures as those described earlier.[21] ^1H NMR spectra were measured by accumulation of 1000 scans at a relaxation time of 2 s on a Bruker ARX 300 MHz spectrometer, using $CDCl_3$ (for CD-SS-PGMA), D_2O (for CD, CD-SS-NH_2, and CD-SS-PGEA) or DMSO-d_6 (for CD-SS-Br) as the solvents. The chemical shifts were referred to the solvent peaks, δ = 7.20 ppm for $CDCl_3$ and δ = 4.70 ppm for D_2O, respectively. After the samples were pressed into KBr pellets, the FTIR spectra were measured on a Bio-Rad FTS 135 FT-IR spectrophotometer. Each spectrum was collected by cumulating 64 scans.

Characterization of Polymer/pDNA Complexes. The plasmid (encoding *Renilla* luciferase) mainly used in this work was pRL-CMV (Promega Co., Cergy Pontoise, France), which was cloned originally from the marine organism *Renilla reniformis*. The plasmid DNA (pDNA) was amplified in *Escherichia coli* and purified according to the supplier's protocol (Qiagen GmbH, Hilden, Germany). The purity and concentration of the purified DNA were determined by absorption at 260 and 280 nm and by agrose gel electrophoresis. The purified pDNA was resuspended in tris-EDTA (TE) buffer and kept in aliquots of 0.5 mg/mL in concentration. All polymer stock solutions were prepared at a nitrogen concentration of 10 mM in distilled water. Solutions were filtered via sterile membranes (0.2 μm) of average pore size and stored at 4 °C. Starlike polymers to DNA ratios are expressed as molar ratios of nitrogen (N) in CD-SS-PGEA to phosphate (P) in DNA (or as N/P ratios). The average mass weight of 325 per phosphate group of DNA was assumed. All polymer/pDNA complexes were formed by mixing equal volumes of polymer and pDNA solutions to achieve the desired N/P ratio. Each mixture was vortexed and incubated for 30 min at room temperature.

Each cationic polymer was examined for its ability to bind pDNA through agarose gel electrophoresis using the similar procedures as those described earlier.[21] The polymer/pDNA complexes at various N/P ratios were investigated. Gel electrophoresis was carried out in TAE running buffer (40 mM Tris-acetate, 1 mM EDTA) with a voltage of 110 V for 30 min in a Sub-Cell system (Bio-Rad Lab, Hercules, CA). DNA bands were visualized and photographed by a UV transilluminator and BioDco-It imaging system (UVP Inc., Upland, CA). To evaluate the heparin-induced release of pDNA from cationic polymer/pDNA complexes in vitro, the procedures similar to those described earlier were used.[27,28]

The particle sizes and zeta potentials of the polymer/pDNA complexes were measured using a Zetasizer Nano ZS (Malvern Instruments, Southborough, MA) using the procedures as described earlier.[19] The polyplex morphology was visualized using an atomic force microscopy (AFM) system with the Dimension 3100 model with a Nanoscope IIIa controller (Veeco, Santa Barbara, CA). The samples were imaged using the tapping mode with setting of 512 pixels/line and 1 Hz scan rate. Image analysis was performed using Nanoscope software after removing the background slope by flatting images.

Cell Viability. The cytotoxicity of the starlike polymers was evaluated using the MTT assay in Hela and HepG2 cell lines. They were cultured in Dulbecco's modified eagle medium (DMEM), supplemented with 10% heat-inactivated fetal bovine serum (FBS), 100 units/mL of penicillin and 100 μg/mL of streptomycin at 37°C, under 5% CO_2, and 95% relative humidity atmosphere. The cells were seeded in a 96-well microtiter plate at a density of 10^4 cells/well and incubated in 100 μL of DMEM/well for 24 h. The culture media were replaced with fresh culture media containing 10 μL polyplex solutions at various N/P ratios, and the cells were incubated for 24 h. Then, 10 μL of sterile-filtered MTT stock solution in PBS (5 mg/mL) was added to each well, reaching a final MTT concentration of 0.5 mg/mL. After 5 h, the unreacted dye was removed by aspiration. The produced formazan crystals were dissolved in DMSO (100 μL/well). The absorbance was measured using a Bio-Rad Model 680 Microplate Reader (UK) at a wavelength of 570 nm. The cell viability (%) relative to control cells cultured in media without polymers was calculated from $[A]_{test}/[A]_{control} \times 100\%$, where $[A]_{test}$ and $[A]_{control}$ are the absorbance values of the wells (with the polymers) and control wells (without the polymers), respectively. For each sample, the final absorbance was the average of those measured from six wells in parallel.

Transfection Assay. Transfection assays were performed firstly using plasmid pRL-CMV as the reporter gene in Hela and HepG2 cell lines in the presence of serum. In brief, the cells were seeded in 24-well plates at a density of 5×10^4 cells in the 500 μL of medium/well and incubated for 24 h. The star-shaped polymer/pDNA complexes (20 μL/well containing 1.0 μg of pDNA) at various N/P ratios were prepared by adding the polymer into the DNA solutions, followed by vortexing and incubation for 30 min at room temperature. At the time of transfection, the medium in each well was replaced with 300 μL of fresh normal medium (supplemented with 10% FBS). The complexes were added into the transfection medium and incubated with the cells for 4 h under standard incubator conditions. Then, the medium was replaced with 500 μL of the fresh normal medium (supplemented with 10% FBS). The cells were further incubated for an additional 20 h under the same conditions, resulting in a total transfection time of 24 h. The cultured cells were washed with PBS twice, and lysed in 100 μL of the cell culture lysis reagent (Promega Co., Cergy Pontoise, France). Luciferase gene expression was quantified using a commercial kit (Promega Co., Cergy Pontoise, France) and a luminometer (Berthold Lumat LB 9507, Berthold Technologies GmbH. KG, Bad Wildbad, Germany). Protein concentration in the cell samples was

analyzed using a bicinchoninic acid assay (Biorad Lab, Hercules, CA). Gene expression results were expressed as relative light units (RLUs) per milligram of cell protein lysate (RLU/mg protein). CD-SS-PGEA-mediated gene transfection was also assessed at their optimal N/P ratios using the enhanced green fluorescent protein (EGFP) pDNA (BD Biosciences, San Jose, CA) as the reporter gene in HepG2 cell lines using the same procedures as those described above. The transfected cells were imaged by using a Leica DMIL Fluorescence Microscope. The percentage of the EGFP positive cells was determined using flow cytometry (FCM, Beckman Coulter, USA).

Determination of Buffering Capacity. The buffering capacity of cationic polymers in the pH range of 2-10 was determined by acid-base titration.[22,23] Polymers were dissolved into 20 mL of saline (0.9% NaCl solution) with a 10 mM amino group concentration. The solutions were titrated with a 0.1 N HCl solution with various volume increments. The pH of all the solutions was measured using a TOLEDO 320 pH meter (METTLER).

Statistical Analysis. All experiments were repeated at least three times. The data were collected in triplicate and expressed as mean ± standard deviations. Error bars represent the standard deviation. The statistical assay was performed using student's *t*-test and the differences were considered statistically significant with $p < 0.05$ with a symbol *.

RESULTS AND DISCUSSION

Introduction of Biocleavable ATRP Initiation Sites onto the β-CD Cores. To prepare biocleavable star-shaped carriers using β-CD as a core via ATRP, it is essential to introduce alkyl halide into β-CD. In this work, some hydroxyl groups of β-CD were converted into bioreducible initiation sites for growing disulfide-linked cationic side chains (Figure 1). The hydroxyl groups of β-CD were first activated in the presence of 1,1′-carbonyldiimidazole (CDI) catalyst to react with cystamine (CA), producing the disulfide bonds-contained β-CD (CD-SS-NH_2). Then, the primary amine groups of CD-SS-NH_2 were activated to react with α-bromoisobutyric acid (BIBA) in the presence of 1-ethyl-3-(3-dimethylaminopropyl) carbodiimide hydrochloride (EDAC) and *N*-hydroxysuccinimide (NHS), producing the bromoisobutylryl-terminated CD (CD-SS-Br) as the multifunctional initiator for subsequent ATRP.

The representative structures of β-CD, CD-SS-NH_2, and CD-SS-Br were first characterized by ^{1}H NMR spectra as shown in Figure 2a–c, respectively. The broad chemical shifts in the wide region of 3.4-4.0 ppm are mainly associated with the inner methylidyne and methylene protons (***a***, CH–O and CH_2–O) on glucose units of β-CD. The chemical shift associated with the unique anomeric proton (***a***′, O–CH–O) of glucose units is at about 4.9 ppm. The signals at δ = 2.67–2.83 ppm and δ = 3.15-3.31 correspond to the methylene protons adjacent to the secondary amine(***c***, CH_2–NH) and disulfide bonds (***b***, CH_2–S–S) of CD-SS-NH_2, respectively. For CD-SS-Br (Figure 2c) the chemical shift at δ = 1.85 ppm is associated with the methyl protons (e, C(Br)–CH_3) of the 2-bromoisobutyryl groups. The signals in the region of 4.19–4.4 ppm are mainly attributable to the hydroxyl protons adjacent to the methylene moieties (***d***, CH2–OH). It has been reported that all the 21 hydroxyl groups of β-CD can be converted into 21 initiation sites.[17,18] When ATRP is carried out from a multifunctional core with a high local concentration of initiation sites, radical–radical coupling of the propagating chains will probably occur and result in gelation. In order to avoid potential gelation and introduce some flexibility onto the starlike cationic polymers for securing a more compact complex structure with DNA, the CD-SS-Br with moderate initiation sites is desired for subsequent star-shaped polymers.[15] In this

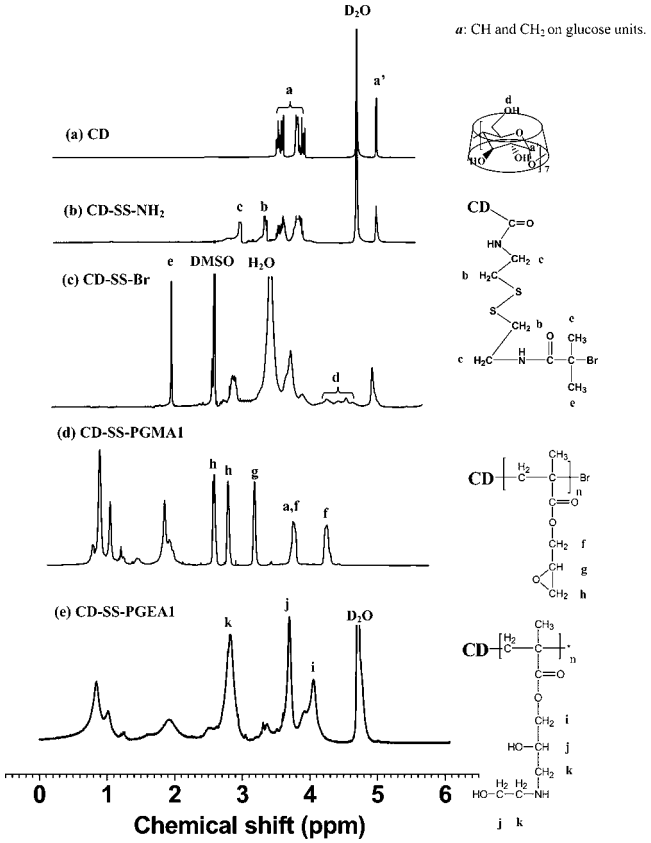

Figure 2. 300 MHz ^{1}H NMR spectra of (a) β-CD in D_2O, (b) CD-SS-NH_2 in D_2O, (c) CD-SS-Br in DMSO, (d) CD-SS-PGMA1 in $CDCl_3$, and (e) CD-SS-PGEA1 in D_2O.

work, based on the area ratio of peak ***e*** and peak ***a***′, it was calculated that the degree of alkyl halide substitution of the hydroxyl groups on the outside surface of CD was determined to be about 4.0, indicating that every CD-SS-Br core possessed about 4 ATRP initiation sites. Such CD-SS-Br with moderate initiation sites can avoid potential gelation during ATRP. In addition, the concentration of initiation sites can be controlled using the activation ratios of hydroxyl groups and cystamine feed ratios, which was consistent with the earlier reports.[21,25] But it should be noted that the hydroxyl groups of CD were randomly or unselectively activated, which probably could handicap fundamental studies and/or applications in contrast with monodisperse systems.[29,30]

Figure 3 shows the FTIR spectra of (a) pristine β-CD, (b) CD-SS-NH_2, and (c) CD-SS-Br. The typical bands at about 1034 cm^{-1} (peak 1), 1083 cm^{-1} (peak 2), and 1155 cm^{-1} (peak 3) were mainly associated with C–H and C–O stretching vibrations of β-CD. In comparison with that of β-CD, the new characteristic peaks at about 1560 cm^{-1} (peak 4, υ_{N-H}) and 1700 cm^{-1} (peak 5, $\upsilon_{O-C(=O)-NH}$) were associated with the amide absorption bands of introduced cystamine species of CD-SS-NH_2. Peak 5 was associated with the linkage (O–C(=O)–-NH) between β-CD and cystamine. For CD-SS-Br, the strong new peak at 1650 cm^{-1} was associated with the linkage (NH–C(=O)–C) between the introduced cystamine and the 2-bromoisobutyryl groups. The FTIR results were consistent with those of ^{1}H NMR (Figure 2).

In addition, CD-SS-NH_2 and CD-SS-Br were also characterized by X-ray photoelectron spectroscopy (XPS). Their representative C 1s spectra were shown in Figures 4a, and 4b,

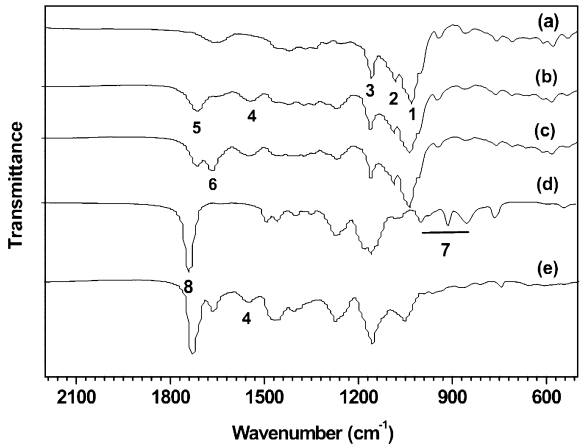

Figure 3. FTIR spectra of (a) β-CD (peak 1, 1034 cm^{-1}, peak 2, 1083 cm^{-1}, and peak 3, 1155 cm^{-1}), (b) CD-SS-NH_2 (peak 4, 1560 cm^{-1}, υ_{N-H}, and peak 5, 1700 cm^{-1}, $\upsilon_{O-\underline{C(=O)}-NH}$), (c) CD-SS-Br (peak 6, 1650 cm^{-1}, $\upsilon_{NH-\underline{C(=O)}-C}$), (d) CD-SS-PGMA1 (peaks 7, 815–950 cm^{-1}, and peak 8, 1725 cm^{-1}, $\upsilon_{O-\underline{C=O}}$), and (e) CD-SS-PGEA1(peak 4, 1560 cm^{-1}, υ_{N-H}).

respectively. The C 1s core-level spectrum of CD-SS-NH_2 (or CD-SS-Br) can be curve-fitted by four peak components with binding energies (BE's) at about 284.6, 285.4, 286.2, and 287.6 eV, attributable to the C–H, C–N, C–O/C–S (or C-O/C–S/C–Br for CD-SS-Br), and O–C–O (or O–C–O/NH–C=O for CD-SS-Br) species, respectively. The C-N and C-S peak components were associated with the cystamine species of CD-SS-NH_2 and CD-SS-Br. The corresponding S 2p (with BE at about 164 eV) and N 1s (with BE at about 399 eV) core-level spectra of SS-CD-NH_2 were shown in Figure 4a′ and a″, respectively. The corresponding Br 3d core-level spectrum (with BE at about 69 eV) of SS-CD-Br was shown in Figure 4b′. The above XPS results also clearly confirmed the successful preparation of CD-SS-NH_2 and CD-SS-Br.

Synthesis and Characterization of Biocleavable CD-SS-PGEA Carriers. CD-SS-PGMA was subsequently synthesized via ATRP of GMA from CD-SS-Br (Figure 1). CD-SS-PGMA with different lengths of PGMA arms can be synthesized by varying the ATRP time. Table 1 summarized the GPC results of CD-SS-PGMA1 (from 5 min of ATRP), CD-SS-PGMA2 (from 10 min of ATRP), and CD-SS-PGMA3 (from 30 min of ATRP). With the increase in reaction time from 5 to 30 min, the M_n of CD-SS-PGMA from GPC increased from 1.69×10^4 to 3.55×10^4 g/mol. The total number of GMA repeat units per arm increased accordingly from 21 to 51, based on the assumption of 4 initiation sites out of every CD-SS-Br core (Table 1). In addition, the polydispersity indexes (PDIs) of CD-SS-PGMAs were comparable to that of CD-SS-Br, indicating that the ATRP of GMA is well-controlled. The ethanolamine (EA)-functionalized

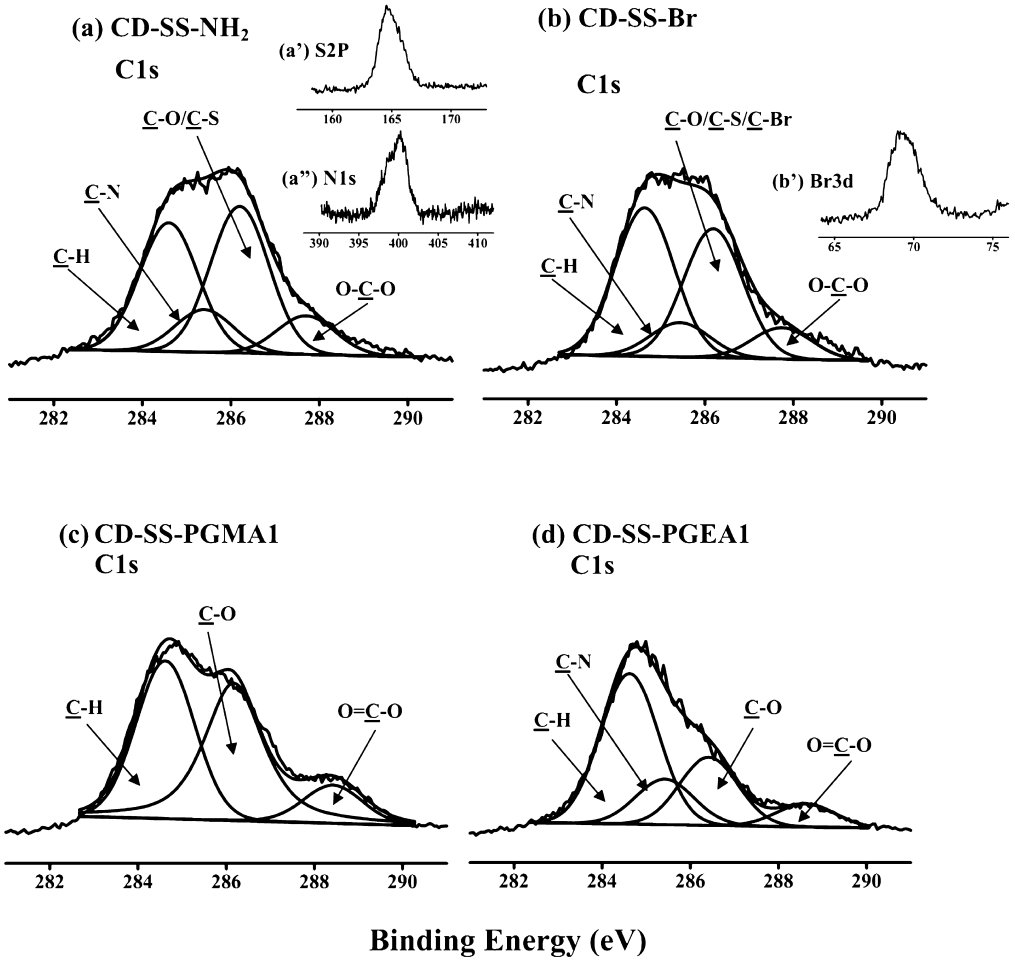

Figure 4. XPS C 1s spectra of (a) CD-SS-NH_2, (b) CD-SS-Br, (c) CD-SS-PGMA1, and (d) CD-SS-PGEA1; (a′) S 2p core-level and (a″) N 1s core-level spectra of CD-SS-NH_2; and (b′) Br 3d core-level spectrum of CD-SS-Br.

dx.doi.org/10.1021/am302249x | ACS Appl. Mater. Interfaces 2013, 5, 703–712

Table 1. Characterization of the Biocleavable Star-Shaped Cationic Polymers

sample	reaction time (min)	M_n (g/mol)[c]	PDI[c]	monomer repeat units per side chain[d]
CD-SS-Br[a]		3.11×10^3	1.32	
CD-SS-PGMA1[b]	5	1.69×10^4	1.35	21
CD-SS-PGMA2[b]	10	2.76×10^4	1.45	39
CD-SS-PGMA3[b]	30	3.55×10^4	1.47	51

[a]CD-SS-Br possesses about four initiation sites. [b]Synthesized using a molar feed ratio [GMA (4 mL)]:[CuBr]:[PMDETA] of 100:1:1.5 at room temperature in 6 ml of DMSO containing 0.2 g of CD-SS-Br. [c]Determined from GPC results. PDI = weight average molecular weight/number average molecular weight, or M_w/M_n. [d]Determined from M_n and the molecular weights of CD-SS-Br (3.11 × 103 g/mol) and GMA (157 g/mol).

CD-SS-PGMA derivatives with flanking cationic secondary amine and nonionic hydrophilic hydroxyl groups were prepared via the ring-opening reaction of the pendant epoxide groups of PGMA arms with the amine moieties of EA to produce the CD-SS-PGEA vectors (Figure 1).

The typical 1H NMR spectra of CD-SS-PGMA1 and CD-SS-PGEA1 were shown in panels d and e in Figure 2, respectively. For CD-SS-PGMA, the signals at δ = 3.8 and 4.3 correspond to the methylene protons adjacent to the oxygen moieties of the ester linkages (***f***, $\underline{CH_2}$−O−C═O) of PGMA arms. The peaks at δ = 3.2 ppm (***g***) and δ = 2.63 and 2.84 ppm (***h***) could be assigned to the protons of the epoxide ring. The peaks at δ = 3.2 (g) and δ = 2.63 and 2.84 (***h***) can be assigned to the protons of the epoxide ring. The ratio of peak areas of peak ***f*** and peak ***g*** is about 1:2, indicating that the epoxy groups in the PGMA remained intact throughout ATRP, which was consistent with the earlier reports.[22,23] The signals associated with the CD core became less obvious, due to the minor contribution of CD to the overall star polymer structure. After the ring-opening reactions of PGMA with EA, the peaks (***g***,***h***) associated with the epoxide rings disappeared completely (Figure 2(***e***)). The peaks (***f***, $\underline{CH_2}$−O−C═O) at δ = 3.8 and 4.3 shifted to one position at δ = 3.95 (***i***). The new peak at δ = 2.7 ppm was mainly attributable to the methylene protons (***k***, NH−$\underline{CH_2}$). The strong peak at δ = 3.7 ppm was associated with the $\underline{CH}$−OH methylidyne and O−$\underline{CH_2}$ methylene protons (***j***). The area ratio of peak ***j*** and peaks ***k***,***i*** is about 4:5, indicating that all oxirane rings of PGMAs were completely opened by excess EA under the present reaction conditions, which was consistent with the earlier reports.[22,23] Based on the molecular weights of EA (61 g/mol) and GMA (142 g/mol), the molecular weight of the repeat units of CD-SS-PGEA was increased to be 203 g/mol. The corresponding M_n values of CD-SS-PGEA1 (from about 21 GMA repeat units per arm, Table 1), CD-SS-PGEA2 (from about 39 GMA repeat units per arm, Table 1), and CD-SS-PGEA 3 (from about 51 GMA repeat units per arm, Table 1) are estimated to be 2.20×10^4, 3.71×10^4, and 4.79×10^4 g/mol, respectively.

The representative FTIR spectra of CD-SS-PGMA1 and CD-SS-PGEA1 are shown in panels c and d in Figure 3, respectively. The FT-IR spectra of CD-SS-PGMA1 show the typical absorption bands (peaks 7, 815−950 cm^{-1}) of the epoxy rings and (peak 8, 1725 cm^{-1}) of ester linkages of PGMA. After the ring-opening reactions of PGMA with EA, the absorption bands (peaks 7) associated with the epoxide rings disappeared in the FTIR spectrum of CD-SS-PGEA1, where the peak 4 at about 1560 cm^{-1} was mainly associated with amide absorption of PGEA arms. The FTIR results also indicated that PGMAs were sucessfully opened by EA.

The representative XPS C 1s spectra of CD-SS-PGMA1 and CD-SS-PGEA1 were shown in panels c and d in Figure 4, respectively. The C 1s core-level spectrum of CD-SS-PGMA1 can be curve-fitted into three peak components with BE's at about 284.6, 286.2, and 288.4 eV, attributable to the C−H, C−O, and O═C−O species, respectively. After the ring-opening reactions, the C 1s spectral line shape of CD-SS-PGEA1 is significantly different from the corresponding spectral line shape of the original CD-SS-PGMA1. The C 1s core-level spectrum of CD-SS-PGEA1 can be curve-fitted into four peak components with BEs at about 284.6, 285.5, 286.2, and 288.4 eV, attributable to the C−H, C−N, C−O, and O═C−O species, respectively. The area ratio of [C−O]/[C−N] was about 1.5, consistent with the chemical structure of PGEA arms. The results from XPS were fairly in agreement with those obtained from ^{1}H NMR.

Biophysical Characterization of Cationic Vector/pDNA Complexes. A successful gene delivery system requires that pDNA must be condensed by polycation into nanoparticles small enough to facilitate cellular uptake. The DNA condensation capability is a prerequisite for polymeric gene vectors. In this work, the ability of the star-shaped cationic polymers to condense pDNA into particulate structures was confirmed by agarose gel electrophoresis, and particle size and zeta potential measurements, as well as AFM imaging.

The formation of the polymer/pDNA complexes was first analyzed by their electrophoretic mobility on an agarose gel at various N/P ratios. Figure 5A showed the gel retardation results of the cationic CD-SS-PGEA polymer/pDNA complexes with increasing N/P ratios, in comparison with that of the branched PEI(25 kDa)/pDNA complexes. All CD-SS-PGEAs can compact pDNA completely within the N/P ratio of 2.0, similar to that of the control PEI.

The particle sizes and surface charges of complexes are important factors in modulating their cellular uptake. The (a) particle size and (b) zeta potential of the cationic polymer/pDNA complexes at various N/P ratios were shown in Figure 6. All the cationic star polymers can efficiently compact pDNA into small particles and showed decreased particle size with increasing N/P ratios. At the N/P ratio of 2.0, loose large aggregates were formed because of the lower amount of cationic polymers. At higher N/P ratios, all vectors condense pDNA into nanoparticles in the diameter range of 100−150 nm. These complexes within this size range can readily undergo endocytosis.[27] Figure 5B showed the representative AFM images of the CD-SS-PGEA1/pDNA complexes at the ratio of 10. Their sizes were within the diameter range of 100 to 200 nm. The result is consistent with that obtained from particle size measurement through dynamic light scattering (Figure 6a). The images also clearly reveal that the compacted complexes existed uniformly in the form of nanoparticles. Zeta potential, an indicator of surface charges on the polymer/pDNA nanoparticles, is another important factor affecting cellular uptake of the complexes. A positively charged surface allows electrostatic interaction with negatively charged cell surfaces and facilitates cellular uptake. As indicated in Figure 6b, the complex surface charge became positive upon the complete self assembly of polycation and pDNA. The positive net surface charge would produce good affinity for anionic cell surfaces.

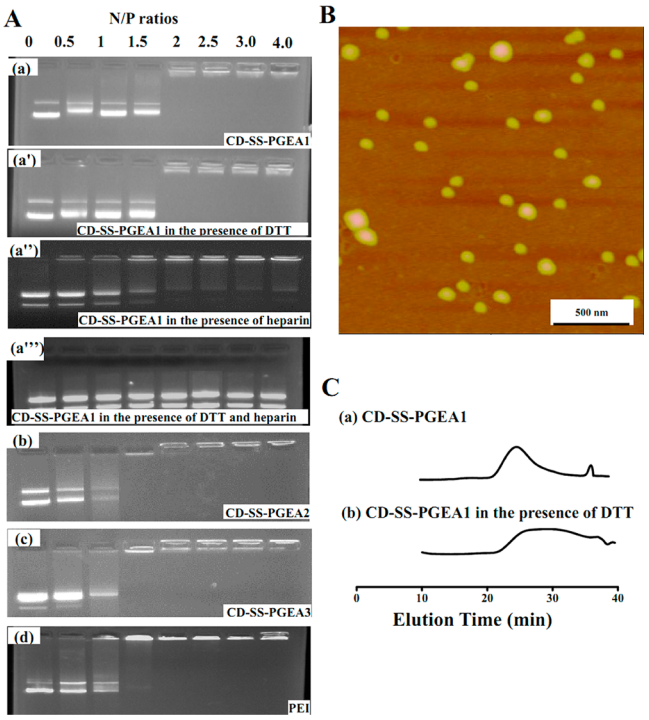

Figure 5. (A) Electrophoretic mobility of pDNA in the complexes of the cationic polymers ((a) CD-SS-PGEA1, (a′) CD-SS-PGEA1 in the presence of 10 mM DTT where the incubation time was 30 min, (a″) CD-SS-PGEA1 in the presence of heparin as the counter polyanion, (a‴) CD-SS-PGEA1 in the presence of 10 mM DTT and heparin where the incubation time was 30 min, (b) CD-SS-PGEA2, (c) CD-SS-PGEA3, (d) PEI) at various N/P ratios. (B) AFM image of the CD-SS-PGEA1/pDNA complexes at a ratio of 10. (C) aqueous GPC traces obtained for (a) CD-SS-PGEA1 and (b) CD-SS-PGEA1 in the presence of 10 mM DTT, where the incubation time with DTT was 1 h.

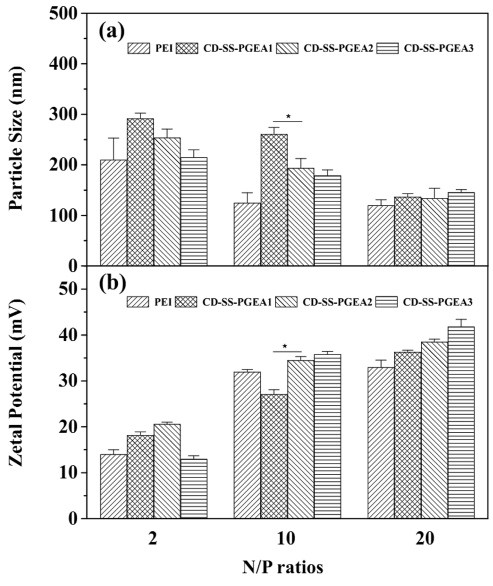

Figure 6. (a) Particle size and (b) zeta potential of the CD-SS-PGEA/pDNA and PEI/pDNA complexes at various N/P ratios. (mean ± SD, n = 3).

Bioreducible Properties. The disulfide bridge linkages between PGEA side chains and CD backbones can make CD-SS-PGEA reductively breakable under reducible conditions. To demonstrate the responsiveness, CD-SS-PGEA was treated with 10 mM of DL-dithiothreitol (DTT), analogous to the intracellular redox potential.[24,25] Such DTT-induced degradation of the disulfide-linked CD-SS-PGEA was demonstrated using GPC analysis (Figure 5C). After incubation with DTT for 1 h, the molecular weight of CD-SS-PGEA decreased substantially. The significant differences in the aqueous GPC traces of CD-SS-PGEA1 before and after the treatment with DTT clearly showed that the disulfide-linked CD-SS-PGEA was responsive to the reductive agent.

Such reducible responsiveness may also have significant effects on pDNA release from the complexes under intracellular reducible conditions. The release of pDNA from the CD-SS-PGEA/pDNA complexes was studied with or without heparin (a competitor anionic sulfated sugar as the model counter polyanion[28,31,32]) under the presence or absence of DTT (Figures 4 and 5(a to a‴)). As shown in Figures 4 and 5(a″), after 30 min incubation at 37°C with heparin in the absence of DTT, the CD-SS-PGEA formulations could barely release pDNA from their complexes. On the other hand, the substantially heparin-induced release was observed in the complexes after 30 min incubation in the presence of DTT (Figure 5A(a‴)). The rapid release of pDNA from the CD-SS-PGEA/pDNA complex under the reducible condition indicated that the cleavage of the PGEA side chains from the CD backbone could lead to the unstable complexes. Such unstable complexes were readily decondensed via interexchange with counter polyanions to induce pDNA release. In addition, without addition of polyanions, no obvious pDNA release was observed in the presence of DTT (Figure 5A(a′)), indicating that under the absence of polyanion competitors, the cleavable PGEA side chains in the unstable complexes still could interact with DNA. Such phenomenon was consistent with the earlier report.[25,31] In fact, varieties of negatively charged macromolecules or cellular components (such as mRNA, sulfated sugars, and nuclear chromatin) exist in cells,[28,31] which can act as competitors to induce pDNA release. The biocleavable nature of CD-SS-PGEAs may greatly facilitate pDNA release in cells, and in turn, could modulate the gene expression in vitro or in vivo.

Cell Viability Assay. A successful delivery system should have high transfection efficiency and compromised toxicity. The cell viability of the polymer/pDNA complexes as a function of N/P ratio was evaluated in the (a) Hela and (b) HepG2 cells by using MTT assay (Figure 7). The N/P ratio had a profound impact on the cytotoxicity of complexes. The cell viability of all polymer/pDNA complexes was observed to decrease with increasing N/P ratios. At higher N/P ratios, the transfection formulation contained also free polymer, besides the compact and positively charged polymer/pDNA complexes. The increased free cationic polymers produced the increasing cytotoxicity. At the same N/P ratio, the cell viability seemed to be highly dependent on the PGEA arm length, CD-SS-PGEA3 with the longest PGEA arms seems to be the most toxic. It was well-known that the cytotoxicity of polycations increases with the molecular weight.[27] The cytotoxicity of CD-SS-PGEAs could be controlled by adjusting the length of the PGEA side chains. In comparison with the CD-SS-PGEA-mediated complexes, the control PEI/pDNA complexes exhibited much higher cytotoxicity. The uniform nonionic hydrophilic hydroxyl groups in PGEAs probably benefited shielding the harmful charges of the cationic carriers.[22] In addition, the biocleavable short PGEA arms were readily

dx.doi.org/10.1021/am302249x | ACS Appl. Mater. Interfaces 2013, 5, 703−712

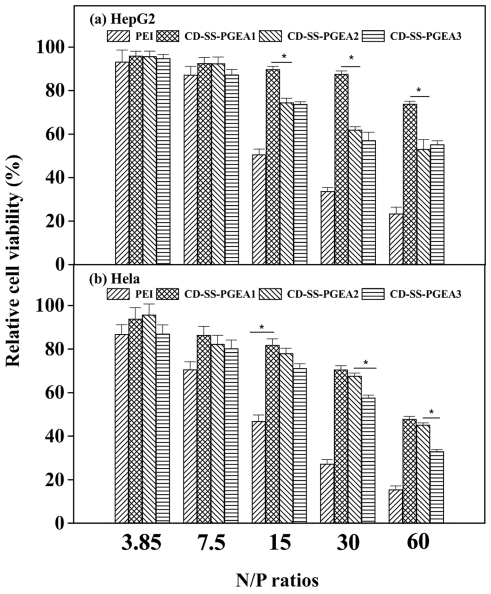

Figure 7. Cell viability of polymer/pDNA complexes at different N/P ratios in (a) HepG2 and (b) Hela cell lines.

detached from the CD core in the intracellular environment after cellular uptake. Such fast degradation of CD-SS-PGEA vectors may also contribute to their lower cytotoxicity.

In vitro Gene Transfection Assay. The in vitro gene transfection efficiency of the cationic polymers/pDNA complexes was first assessed using luciferase as a gene reporter in Hela and HepG2 cell lines in the complete serum media. Figure 8A showed the gene transfection efficiency mediated by CD-SS-PGEAs in comparison with those of PEI (25 kDa) at various N/P ratios and that of linear PGEA derived from PGMA homopolymer ($M_n \approx 9.5 \times 10^3$; GMA units ~67[23]) at its optimal N/P ratio of 20. The transfection efficiency generally first increases at lower N/P ratios and then decreases slightly with the increase in N/P ratios. At lower N/P ratios, pDNA cannot be condensed efficiently by the cationic polymers, and the resultant loose polymer/pDNA complex cannot enter the cell easily. At higher N/P ratios, the transfection formulation contains also free polymer. Because of the presence of an increasing amount of free cationic polymers with the increase in N/P ratios, the increasing cytotoxicity may result in a reduction in the transfection efficiency. The transfection efficiency mediated by naked pDNA was much lower ($<1 \times 10^5$ RLU/mg protein), which was consistent with the earlier report.[2] No any transfection efficiency was observed for CD-SS-PGEA alone.

The transfection efficiency mediated by CD-SS-PGEA1 was much lower than those mediated by other CD-SS-PGEAs, especially at lower N/P ratios in both cell lines. At higher N/P ratios, the relative high cytotoxicity of CD-SS-PGEA3/pDNA resulted in a larger reduction in the transfection efficiency. This observation indicated that the optimal transfection efficiency for CD-SS-PGEAs was dependent on the side lengths of PGEA arms. With the increase in the arm length of PGEA of CD-SS-PGEAs, their optimal transfection efficiency generally increases in both cell lines. The long PGEA arms can increase the binding ability and complex stability, probably leading to much higher transfection efficiency. In addition, in both cell lines, the optimal transfection efficiencies mediated by CD-SS-PGEAs exhibited much higher gene transfection efficiency than those mediated by PGEA and PEI (25KDa). The above results indicated that the star polymers composed of biocompatible CD cores and disulfide-linked low-molecular-weight PGEA arms can enhance gene transfection efficiency. As mentioned

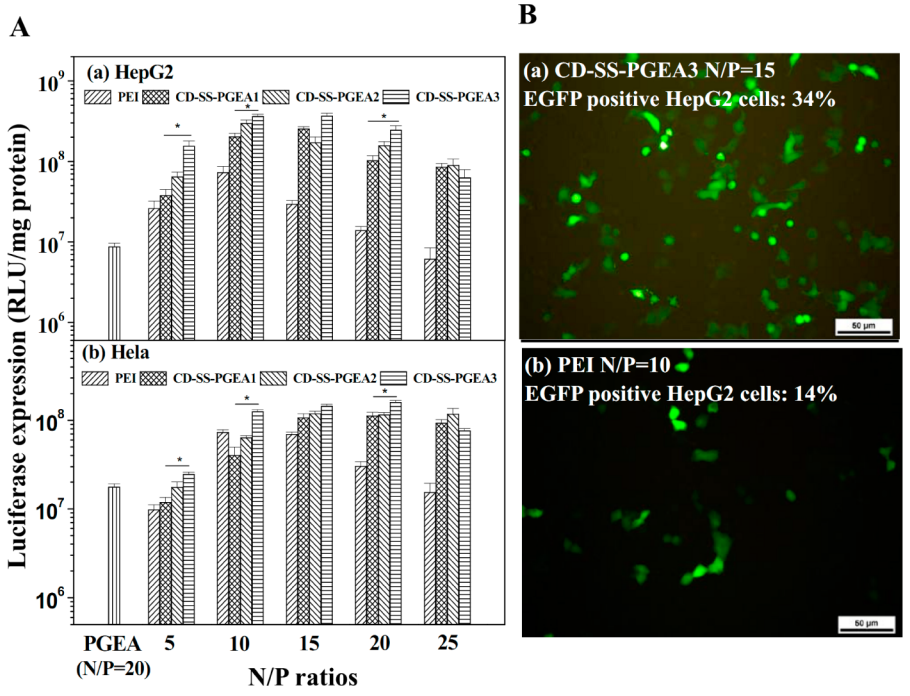

Figure 8. In vitro gene transfection efficiency of the CD-SS-PGEA/pDNA complexes (A) at various N/P ratios in comparison with those mediated by PEI (25 kDa) and PGEA (at its optimal N/P ratio of 20) in (a) HepG2 and (b) Hela cell lines (mean ± SD, $n = 3$), and representative images (B) of EGFP expression mediated by (a) CD-SS-PGEA3 (at the optimal N/P ratio of 15) and (b) PEI (25 kDa) (at the optimal N/P ratio of 10) in HepG2 cells.

above, the disulfide bridge linkages were responsive to the reductive agent, making CD-SS-PGEA breakable. Under intracellular reducible conditions, such responsiveness could produce the unstable complexes, which were readily decondensed to greatly facilitate pDNA release from the complexes and benefit the resultant gene expression.

In an attempt to confirm the gene delivery capability of biocleavable gene vectors, direct visualization of gene expression of enhanced green fluorescent protein (EGFP) in HepG2 cells was also performed under fluorescence microscopy. Plasmid pEGFP-N1 encoding GFP was delivered to examine the EGFP expression. Representative images of EGFP gene expression mediated by CD-SS-PGEA3 at the optimal N/P ratio of 15 and PEI (25 kDa) at the optimal N/P ratio of 10 were shown in Figure 8B. Significantly stronger fluorescence signals were observed in delivering plasmid EGFP mediated by CD-SS-PGEA3. In the case of PEI-mediated gene transfection, significantly less fluorescence was observed in the field of vision. The percentages (determined using flow cytometry[21]) of the EGFP-positive HepG2 cells for CD-SS-PGEA3 (N/P = 15) and PEI (N/P = 10) were 34% and 14%, respectively. The above results suggested the HepG2 cells treated with CD-SS-PGEA3/pEGFP complexes showed much higher expression levels than those mediated by PEI, which was consistent with the results of luciferase expression (Figure 8A). All the transfection results also indicated that CD-SS-PGEA vectors may have great ability to transfect those difficult-to-transfect cell lines such as HepG2.

Buffering Capacity. After cellular entry via endocytosis, the polymer/plasmid complexes were transported into the lysosome. Efficient escape from endosomes is one of the most important factors to be considered for the design of gene delivery vehicles. This event is associated with the buffering capacity of gene vectors, in which vectors undergo from extracellular environment to endosomal acid environment.[32−35] By disrupting the endosomal membrane, polycations with high buffering capacity can mediate efficient escape from endosome to cytosol triggered by the acidic environment of endosome. The buffering capacity of the cationic polymers is very useful for the endosomal release of pDNA to the cytoplasm. In this study, acid−base titration under the given 10 mM amino group concentration was performed to evaluate the proton-buffering effects of CD-SS-PGEA (Figure 9). CD-SS-PGEA showed significantly higher buffering capacity than PEI (25 kDa), a well known transfection agent for its strong proton-sponge effect.[34]

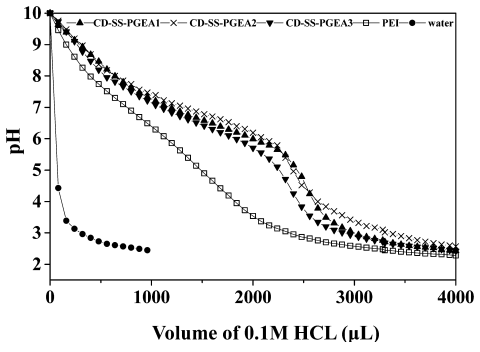

Figure 9. Determination of the buffer capacity of CD-SS-PGEA, PEI, and water by acid-base titration. The cationic polymer solutions with 10 mM amino group concentration were titrated with 0.1 M HCl solution.

This was consistent with our earlier report.[22,23] The local environment of the nonionic hydrophilic hydroxyl groups of PGEA arms may benefit the improvement the buffering capacity, benefiting the endosomal escape of condensed pDNA. In addition, no obvious difference was observed in the buffering capacities of the CD-SS-PGEA vectors in the entire test pH range.

CONCLUSIONS

In summary, the biocleavable star-shaped vectors (CD-SS-PGEAs) consisting of nonionic β-CD cores and disulfide-linked PGEA arms with different lengths were successfully prepared for highly efficient gene delivery. These CD-SS-PGEAs possessed the favorable properties of flexible CD-based star polymers, low toxic PGEA, and reduction-sensitive polymers. The cationic PGEA arms can be readily cleavable from the β-CD cores under reducible conditions. Such biocleavable star-shaped CD-SS-PGEA vectors exhibited good ability to complex pDNA and enhanced gene transfection efficiencies in different cell lines. Thus, the present work demonstrated that properly grafting bioreducible cationic low-toxic PGMA derivative arms from nonionic β-CD cores via ATRP would provide an effective means to construct new gene delivery systems.

AUTHOR INFORMATION

Corresponding Author

*E-mail: xufj@mail.buct.edu.cn.

Notes

The authors declare no competing financial interest.

ACKNOWLEDGMENTS

This work was supported by National Natural Science Foundation of China (Grants 21074007, 51173014, and 51221002), Research Fund for the Doctoral Program of Higher Education of China (projects 20090010120007 and 20120010110007), Program for New Century Excellent Talents in University (NCET-10-0203), SRF for ROCS, SEM and National High Technology Development Program of China (863 Program 2011AA030102).

REFERENCES

(1) De Smedt, S. C.; Demeester, J.; Hennink, W. E. *Pharm. Res.* **2000**, *17*, 113.
(2) Xu, F. J.; Li, H. Z.; Li, J.; Zhang, Z. X.; Kang, E. T.; Neoh, K. G. *Biomaterials* **2008**, *29*, 3023.
(3) Bisht, H. S.; Manickam, D.S.; You, Y.; Oupicky, D. *Biomacromolecules* **2006**, *7*, 1169.
(4) Lin, C.; Zhong, Z. Y.; Lok, M. C.; Jiang, X. L.; Hennink, W. E.; Feijen., J. *J. Control. Release* **2006**, *116*, 130.
(5) Piest, M.; Lin, C.; Mateos-Timoneda, M. A.; Lok, M. C.; Hennink, W. E.; Feijen, J. *J. Control. Release* **2008**, *130*, 38.
(6) Mao, S.; Sun, W.; Kissel, T. *Adv. Drug Delivery Rev.* **2010**, *62*, 12.
(7) Li, W.; Chen, L.; Huang, Z.; Wu, X.; Zhang, Y.; Hu, Q.; Wang, Y. *Org. Biomol. Chem.* **2011**, *9*, 7799.
(8) Ortiz Mellet, C.; García Fernández, J. M.; Benito, J. M. *Chem. Soc. Rev.* **2011**, *40*, 1586.
(9) Guo, J.; Ogier, J. R.; Desgranges, S.; Darcy, R.; O'Driscoll, C. *Biomaterials* **2012**, *33*, 7775.
(10) Srinivasachari, S.; Fichter, K. M.; Reineke, T. M. *J. Am. Chem. Soc.* **2008**, *130*, 4618.
(11) Davis, M. E.; Brewster, M. E. *Nat. Rev. Drug Discov.* **2004**, *3*, 1023.
(12) Díaz-Moscoso, A.; Guilloteau, N.; Bienvenu, C.; Méndez-Ardoy, A.; Blanco, J. L. J.; Benito, J. M.; Gourriérec, L. L.; Giorgio, C.D.;

Vierling, P.; Defaye, J.; Ortiz Mellet, C.; García Fernández, J.M. *Biomaterials* **2011**, *32*, 7263.
(13) Bennevault-Celton, V.; Urbach, A.; Martin, O.; Pichon, C.; Guégan, P.; Midoux, P. *Bioconjugate Chem.* **2011**, *22*, 2404.
(14) Mourtzis, N.; Paravatou, M.; Mavridis, I. M.; Roberts, M. L.; Yannakopoulou, K. *Chem.Eur. J.* **2008**, *14*, 4188.
(15) Xu, F. J.; Zhang, Z. X.; Ping, Y.; Li, J.; Kang, E. T.; Neoh, K. G. *Biomacromolecules* **2009**, *10*, 285.
(16) Georgiou, T. K.; Vamvakaki, M.; Phylactou, L. A.; Patrickios, C. S. *Biomacromolecules* **2005**, *6*, 2990.
(17) Li, J.; Guo, Z.; Xin, J.; Zhao, G.; Xiao, H. *Carbohyd. Polym.* **2010**, *79*, 277.
(18) Guo, Z.; Chen, X.; Xin, J.; Wu, D.; Li, J.; Xu, C. *Macromolecules* **2010**, *43*, 9087.
(19) Xu, F. J.; Zhu, Y.; Liu, F. S.; Nie, J.; Ma, J.; Yang, W. T. *Bioconjugate Chem.* **2010**, *21*, 456.
(20) Xu, F. J.; Ping, Y.; Ma, J.; Tang, G. P.; Yang, W. T.; Kang, E. T. *Bioconjugate Chem* **2009**, *20*, 1449.
(21) Wang, Z. H.; Li, W. B.; Ma, J.; Tang, G. P.; Yang, W. T.; Xu, F. J. *Macromolecules* **2011**, *44*, 230.
(22) Xu, F. J.; Chai, M. Y.; Li, W. B.; Ping, Y.; Tang, G. P.; Yang, W. T. *Biomacromolecules* **2010**, *11*, 1437.
(23) Yang, X. C.; Chai, M. Y.; Zhu, Y.; Yang, W. T.; Xu, F. J. *Bioconjugate Chem.* **2012**, *23*, 618.
(24) Ganta, S.; Devalapally, H.; Shahiwala, A.; Amiji, M. *J. Control. Release* **2008**, *126*, 187.
(25) Wang, Z. H.; Zhu, Y.; Chai, M. Y.; Yang, W. T.; Xu, F. J. *Biomaterials* **2012**, *33*, 1873−1883.
(26) McCarley, R. L. *Annu. Rev. Anal. Chem.* **2012**, *5*, 391.
(27) Xiang, S.; Tong, H.; Shi, Q.; Fernandes, J .C.; Jin, T.; Dai, K.; Zhang, X. *J. Control. Release* **2012**, *158*, 371.
(28) Chen, D.; Ping, Y.; Tang, G. P.; Li, J. *Soft Matter* **2010**, *11*, 655.
(29) Díaz-Moscoso, A.; Gourriérec, L. L.; Gómez-García, M.; Benito, J. M.; Balbuena, P.; Ortega-aballero, F.; Guilloteau, N.; Di Giorgio, C.; Vierling, P.; Defaye, J.; Ortiz Mellet, C.; García Fernández, J. M. *Chem.—Eur. J.* **2009**, *15*, 12871.
(30) Byrne, C.; Sallas, F.; Rai, D. K.; Ogier, J.; Darcy, R. *Org. Biomol. Chem.* **2009**, *7*, 3763.
(31) Kang, H. C.; Kang, H.J.; Bae, Y. H. *Biomaterials* **2011**, *32*, 1193−1203.
(32) Neu, M.; Germershaus, O.; Mao, S.; Voigt, K. H.; Behe, M.; Kissel, T. *J. Control. Release* **2007**, *118*, 370.
(33) Boussif, O.; Lezoualc'h, F.; Zanta, M. A.; Mergny, M. D.; Scherman, D.; Demeneix, B. *Proc. Natl. Acad. Sci. U.S.A.* **1995**, *92*, 7297.
(34) Wang, D. A.; Narang, A. S.; Kotb, M.; Gaber, A. O.; Miller, D. D.; Kim, S. W. *Biomacromolecules* **2002**, *3*, 1197.
(35) Zhang, X. Q.; Wang, X. L.; Huang, S. W.; Zhou, R. X.; Liu, Z. L.; Mao, H. Q. *Biomacromolecules* **2005**, *6*, 341.